Review of Various Approaches and Successes For High Gradients and Q's for TESLA

H. Padamsee, Laboratory of Nuclear Studies, Cornell University, Ithaca, NY 14853

Acknowledgements

This review is based on the work done at Cornell, CEBAF, CERN, Saclay, Los Alamos and Wuppertal. I am grateful to P. Kneisel, W. Weingarten, B. Bonin, and B. Rusnak, R. Roeth and D. Reschke for supplying information. The Cornell work reviewed here consists of two parts. The first is the extensive doctoral dissertation work of J. Graber. The second is a collaborative TESLA effort between Cornell, DESY and FNAL. The following people were involved in the collaboration effort: DESY: P. Schmuser, W. Moller, A. Matheisen, M. Pekeler. FNAL: C. Crawford, H. Edwards, K. Koepke, H. Pfeffer, M. Champion, L. Bartelson, T. Nichols, M. Rushman, Q. Kearns, R. Pasquanelli, M. Kuchnir. CORNELL: J. Kirchgessner, J. Sears, P. Barnes, D. Moffat and M. Tigner.

This work was supported by the National Science Foundation with supplementary support from the US-Japan Collaboration.

Introduction

The goals for TESLA, which are to reach a gradient of 25 MV/m at a Q of 5×10^9, call for a substantial improvement over the present day performance of niobium cavities. As an intermediate step, the goals for the TEST FACILITY, now under construction at DESY, have been selected at the more modest gradient of 15 MV/m at a Q of 3×10^9. The RF frequency chosen for TESLA is 1.3 GHz, the operating temperature is 2 K, and the structures are 9-cells, about 1 meter long. I review here the various approaches that are under investigation at various laboratories to reach these targets and the degree of progress registered with each.

Q Values

Now that CEBAF has tested more than three hundred 5-cell structures, their data[1] are an excellent representation of the state of the art. Figure 1 shows the Q values before the

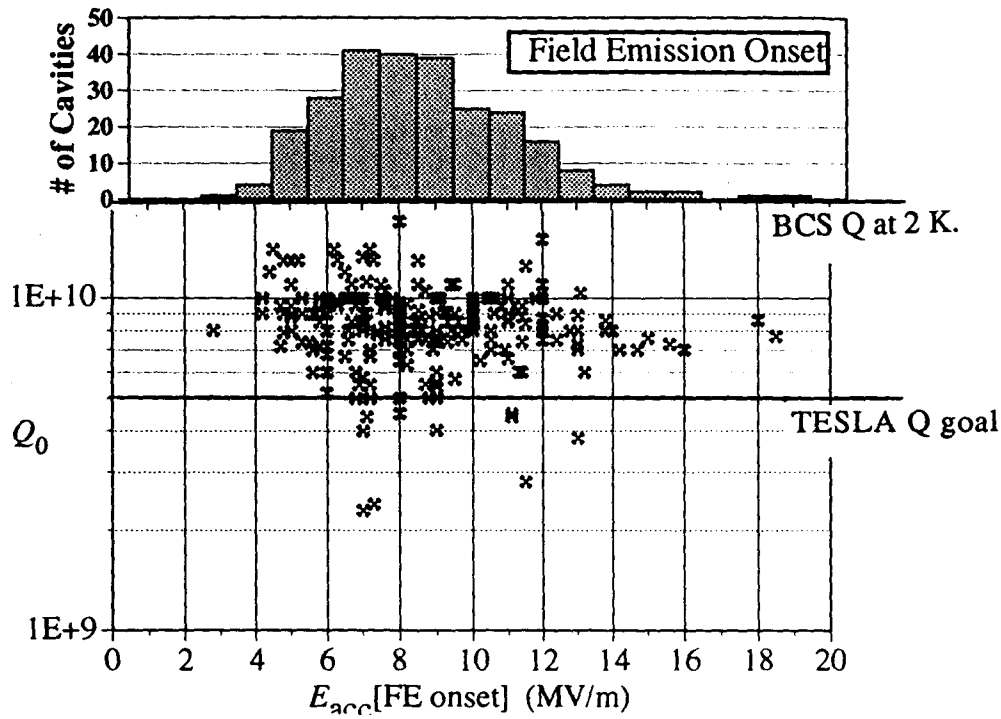

Figure 1: Q values of CEBAF 5-cell structures just before the onset of field emission.

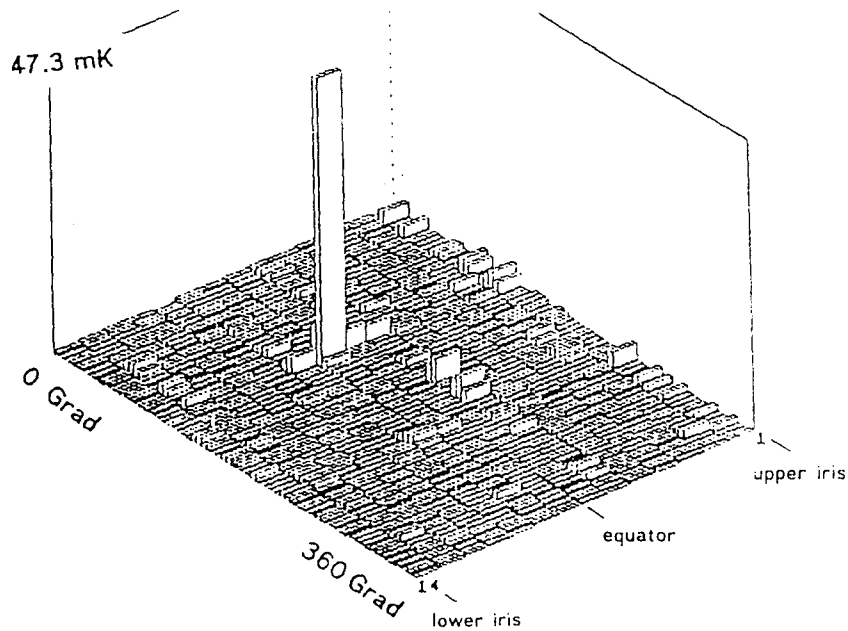

Figure 2: Temperature map from a 1-cell 3 GHz cavity at 1.6 K, showing different sources of residual resistance.

onset of field emission, showing that most cavities regularly exceed the TESLA Q goal below Eacc = 10 MV/m. Some even come close to the BCS Q at 2 K.

Ignoring field emission, what are the dominant loss mechanisms? A detailed temperature map at 1.6 K and 1000 Oersted from a 3 GHz cavity at Wuppertal[2] shows in Figure 2 important types of losses: from one isolated large defect, from several smaller regions of loss in the high magnetic field, and several regions of dielectric losses in the high electric field. The microscopic nature of these lossy sites is far from understood. Where the losses are lowest, the temperature rise translates to a surface resistance of 4 nano-ohms, which is equal to the BCS resistance within the experimental error of 1 nano-ohm. Therefore local temperature based measurements reveal that it is possible with present surface preparation techniques to achieve extremely low residual losses (< 2 nano-ohm) over large parts of the cavity area, equivalent to a $Q > 10^{11}$, which is lower than the BCS Q of 7×10^{10} at this temperature and frequency.

At the maximum fields reached, the CEBAF cavities show in Figure 3 how much the Q falls, primarily due to increased losses from field emission. For TESLA it is clear that field emission is the common enemy for high fields and high Q's. Beyond TESLA, however, it may prove beneficial for higher luminosity to work toward Q values of 10^{11} that appear possible in principle from the thermometry survey of Figure 2. If realized, such Q gains will allow longer RF pulse length, more bunches per pulse and a higher efficiency of AC wall plug power to beam power. But the attention now is focussed toward higher gradients to lower the capital cost of the TESLA in the 0.5 CM energy range.

Towards Higher Gradients

The state of the art in achievable gradients from many laboratories is shown in Figure 4. More than 360 structure test results are included, a very large fraction from CEBAF. The average gradient in the acceptance tests is nearly 10 MV/m, compared the the design value of 5 MV/m for the applications intended by the laboratories. Why do the numbers drop off so sharply above 10 MV/m? There are two major field limiting mechanisms operative here: thermal breakdown and field emission.

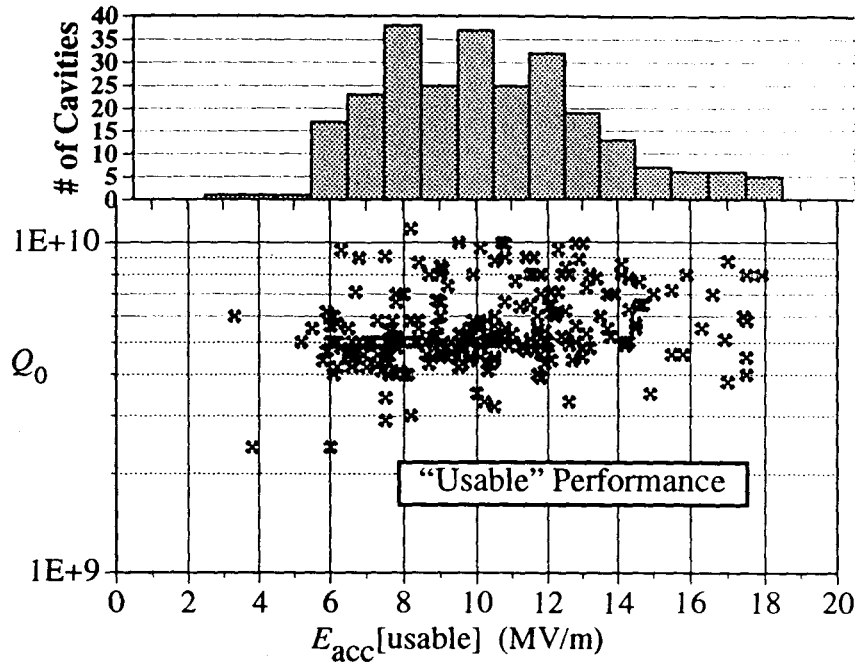

Figure 3: Q values of CEBAF 5-cell structures at the maximum achievable field in the vertical acceptance tests.

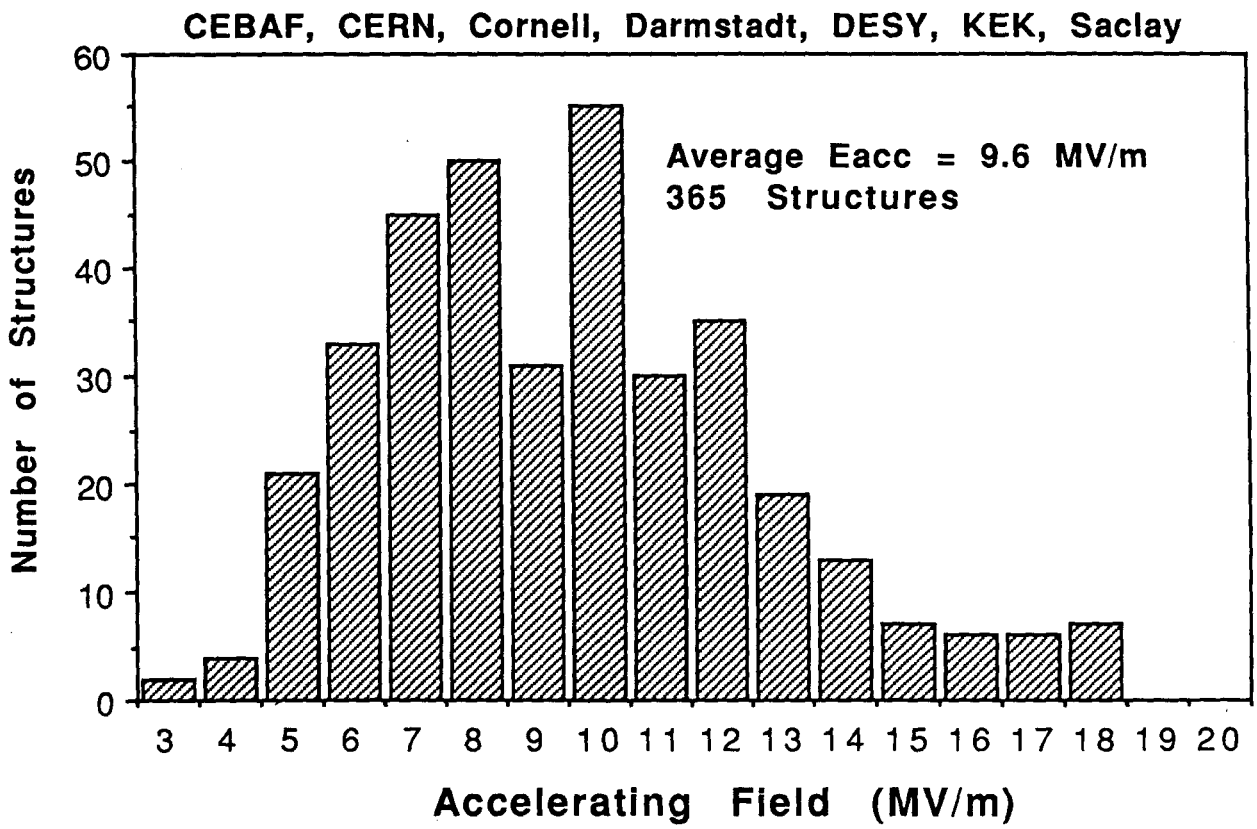

Figure 4: State of the art in gradients for Nb accelerating structures from various laboratories.

Thermal breakdown Limits, Approches to Improvement

Figure 5 shows the nearly gaussian distribution of quench fields for about 100 CEBAF strcutures, The average quench field is Eacc = 13 MV/m (Hpk = 611 Oersted) Clearly the RRR (specified as > 250) is not high enough for TESLA goals. If we desire an average gradient of Eacc = 25 MV/m (Hpk = 1050 Oersted), then roughly speaking we must ask for 3 times greater RRR, i.e. RRR > 750, a daunting challenge. Thermal model calcuations show that the gain is not as fast as square root of RRR[3], so the target should be closer to RRR = 1000.

Fortunately the RRR of Nb delivered by industry has been going up steadily as shown in Figure 6. In the last two years Nb from Russia is available with RRR between 500 and 700. It is important to check whether a new source of Nb for cavities is acceptable. At Cornell and Wuppertal[4], 3 GHz single cell cavities made from Russian Nb (RRR = 700) reached Q values above 10^{10} at low fields, and maximum surface magnetic fields limited by global thermal instability around 1300 Oersted at 3 GHz, or by field emission. It is safe to say that the new Russian Nb does not hold any unpleasant surprises. Whether we can reap the benefits of the higher RRR depends on the outcome of the battle with field emission. The global thermal instability will not be a problem at the lower TESLA frequency of 1.3 GHz. We also hope that U.S. and European suppliers of Nb will rise to the challenge to match Russian high RRR Nb.

Another proven approach is to improve the RRR of industrial Nb by solid state gettering. At least a factor of two can be expected, since the oxygen remaining can be removed. There are recent results from CEBAF that show that even higher gains can be expected. After 4 hours at 1400 C, the RRR of Nb was observed to improve from 300 to 800 for 3 mm thick Nb and to 1200 for 1.5 mm thick Nb [5]. Solid state gettering on 700 RRR Russian Nb gave RRR = 1400[6]. The goal of RRR = 1000 has therefore been proved in principle.

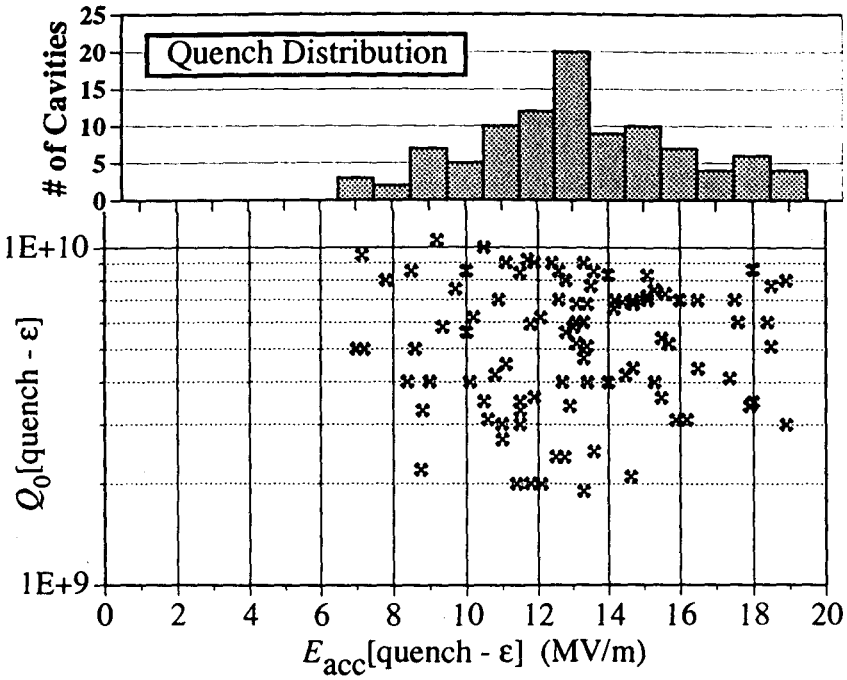

Figure 5: Distribution of quench fields for CEBAF structures made with RRR > 250 (nominal).

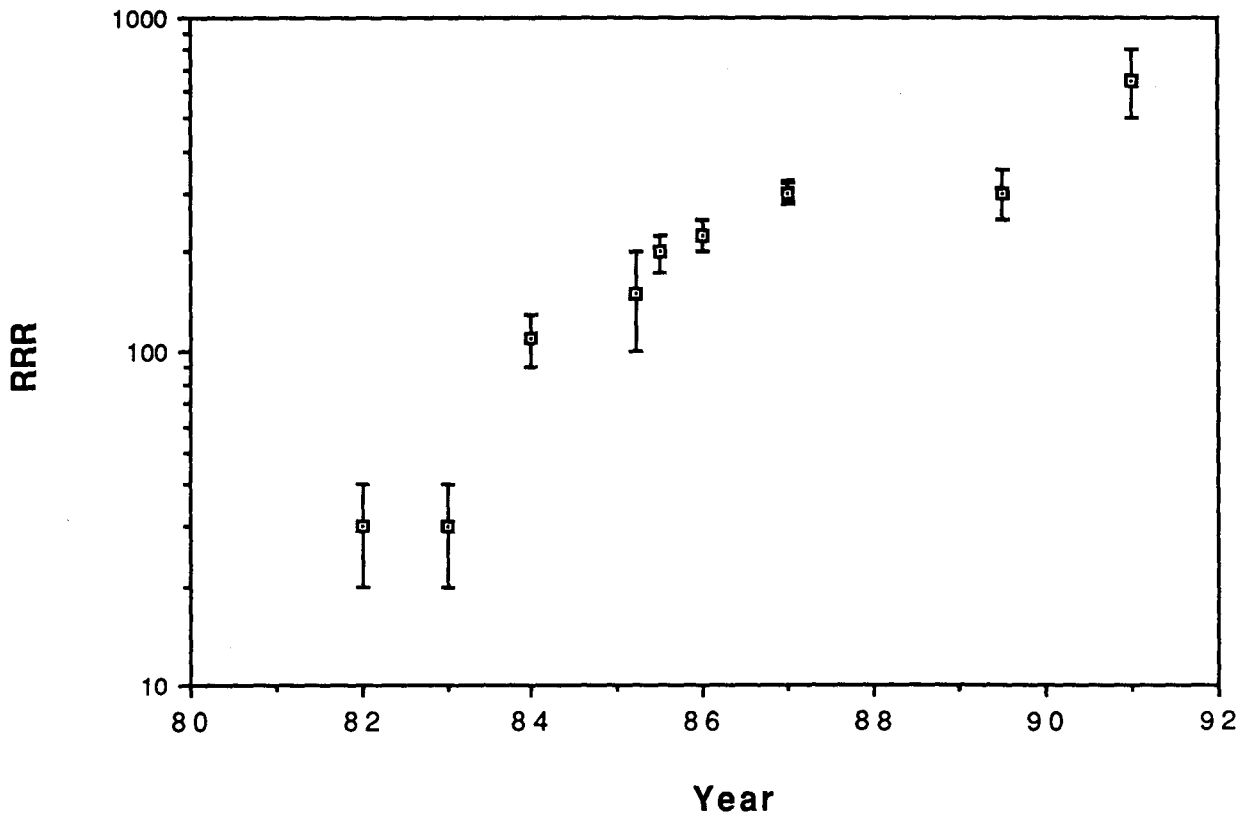

Figure 6: Improvement of RRR with time.

Field Emission - What Do the Present Results Tell Us?

Much progress has been made in the fight against field emission over the last two years, both in terms of better understanding the enemy as well as in defeating it. It is now generally agreed that microparticle contamination, most often conducting particles[7], are the culprits responsible for field emission currents. Better cleanliness in cavity surface preparation, assembly and testing are called for.

Fortunately, one can continue to make gains over field emission by processing. The mechanism of RF processing is now better understood. Several 1-cell 3 GHz accelerator cavities were dissected after locating and processing field emitters[8]. Before processing, emitters were located by mapping the heating caused by the impacting electrons. Temperature maps also confirmed the successful processing of emitters. After dissection, SEM examination of the emitter/processed areas revealed molten craters, foreign element debris and starbursts (Figure 7).

In the "mushroom" cavity at Cornell[9], it is possible to expose a small region of niobium (called the dimple) to a very high RF electric field, and subsequently to examine this region with SEM/EDX for μm size particulates and Auger electron spectroscopy (AES) for nanometer surface layers of foreign elements. In RF tests we successfully exposed the dimple to fields ranging from 50 to 145 MV/m. Subsequently in the SEM we found 5 -10 μm craters of molten niobium, covered with a thin (10-100 Angstrom) layer of foreign elements. Frequently we encountered μm size foreign element debris in various stages of melting in the vicinity of the craters. Surrounding the molten craters, we always found 100 μm diameter starburst shaped spots that appear dark in the SEM, but are invisible in the optical microscope. The distribution of foreign elements found with the Auger exams is shown in Figure 8[10].

The frequent occurrence of iron and chromium suggest that some emitters come from the stainless hardware used in cavity assembly or from the stainless steel vacuum system, while the silicon could come from dust.

The features found in the high electric field region of the mushroom and accelerator cavities suggest the occurrence of a spark (micro-discharge) in the high RF field at the

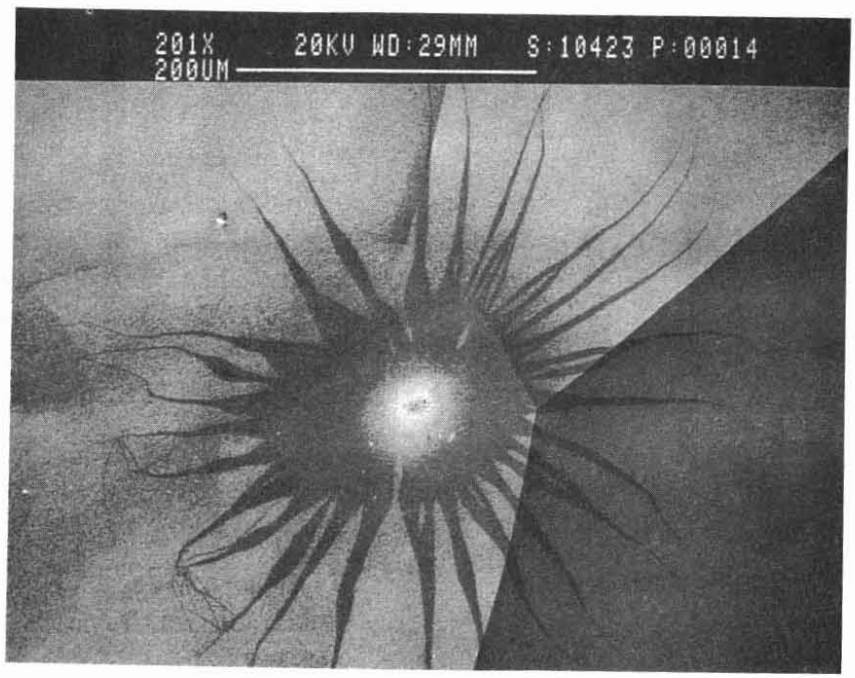

Figure 7: Typical starburst and molten craters found after RF processing of emitters.

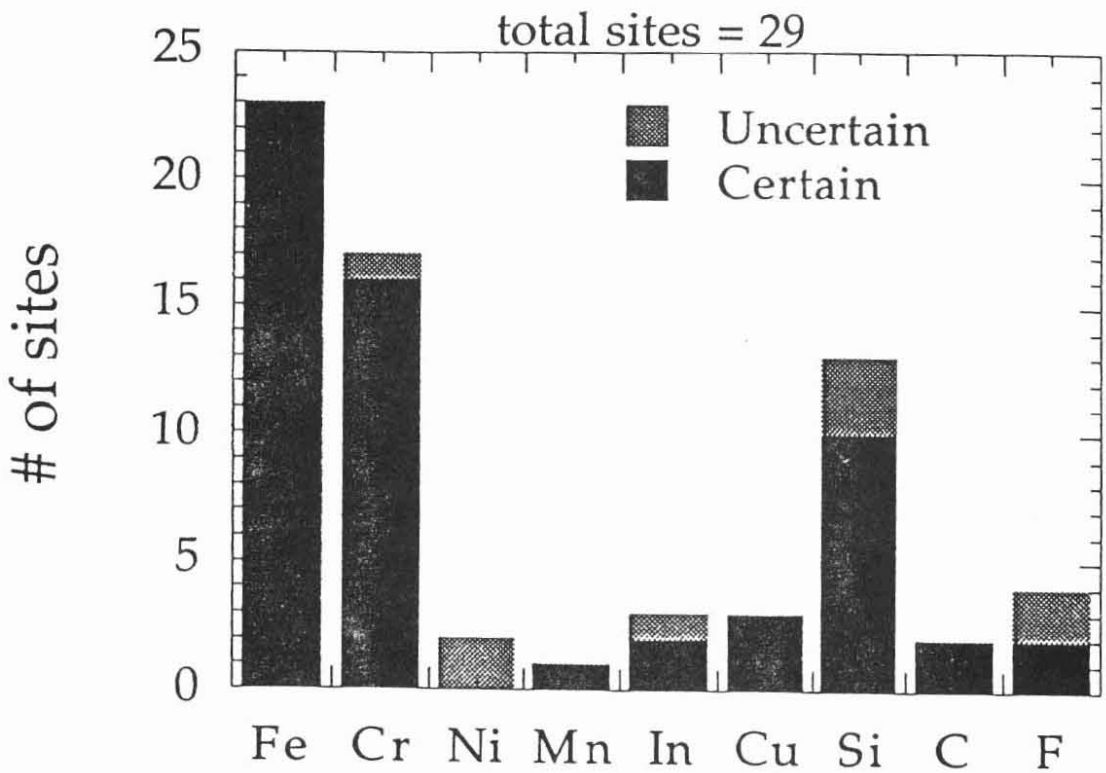

Figure 8: Distribution of foreign elements found on or near molten craters.

microparticle field emission site. The foreign elements found so far indicate that all these sites are metallic particles. We surmise that processing takes place by the explosive mechanism associated with the spark. The activities within the plasma of the spark are presumably responsible for the starburst feature, extending over a region of several hundred microns, while the central molten core is the region where most of the energy during the spark is dissipated. Fragments of foreign material, most likely the root cause of the emission are expelled during the crater formation.

Sufficient evidence has accumulated to prove that the features which result from RF processing, i.e. the craters, debris and starbursts are not very harmful to the Q_0 of the cavity at the level desired for TESLA. In one case, 40 such sites were found with the SEM in a single cell cavity that reached Epk = 72 MV/m. The same cavity operated at CW Epk = 40 MV/m while the Q_0 remained near $1x10^{10}$.

We do not as yet understand what are the physical properties of the microparticles that control the strength of the field emission current, or of the interface between the particles and the base metal. We continue to characterize the emission by the usual Fowler-Nordheim parameters, the field enhancement factor β and the emissive area, S. We observe by various methods, typical β values between 40 and 600, and log(S - m^2) between -8 and -16. DC field emission studies suggest that among the emitters that are present on the surface, there are many more with low β values than with high β values, while the log S values are randomly distributed over a gaussian centered around log(S) = -12[11].

It is possible to reconcile the observed sharp drop off in cavity field values at high gradients with the above observations about β and S, using a simple statistical model[12]. The model takes the emitter density to be random between 0 and 0.3 emitters/cm^2 and also allows for the extinction of emitters that put out high currents (processing)[8]. As shown in Figure 9, the predictions of such a model agree very well with the extensive data set from 1.5 GHz, 5-cell CEBAF cavities, as well as with the data from 100 tests on 1-cell 3 GHz cavities[13]. Even though the area of the CEBAF structure is 20 times larger than the Los Alamos 1-cell test cavity, the model mimics the experimental trends quite well for both sets. Note how there is a 20% chance of reaching CW surface fields of 80 MV/m in single cell S-band cavities, because there is a finite probability that a small area cavity can be free of

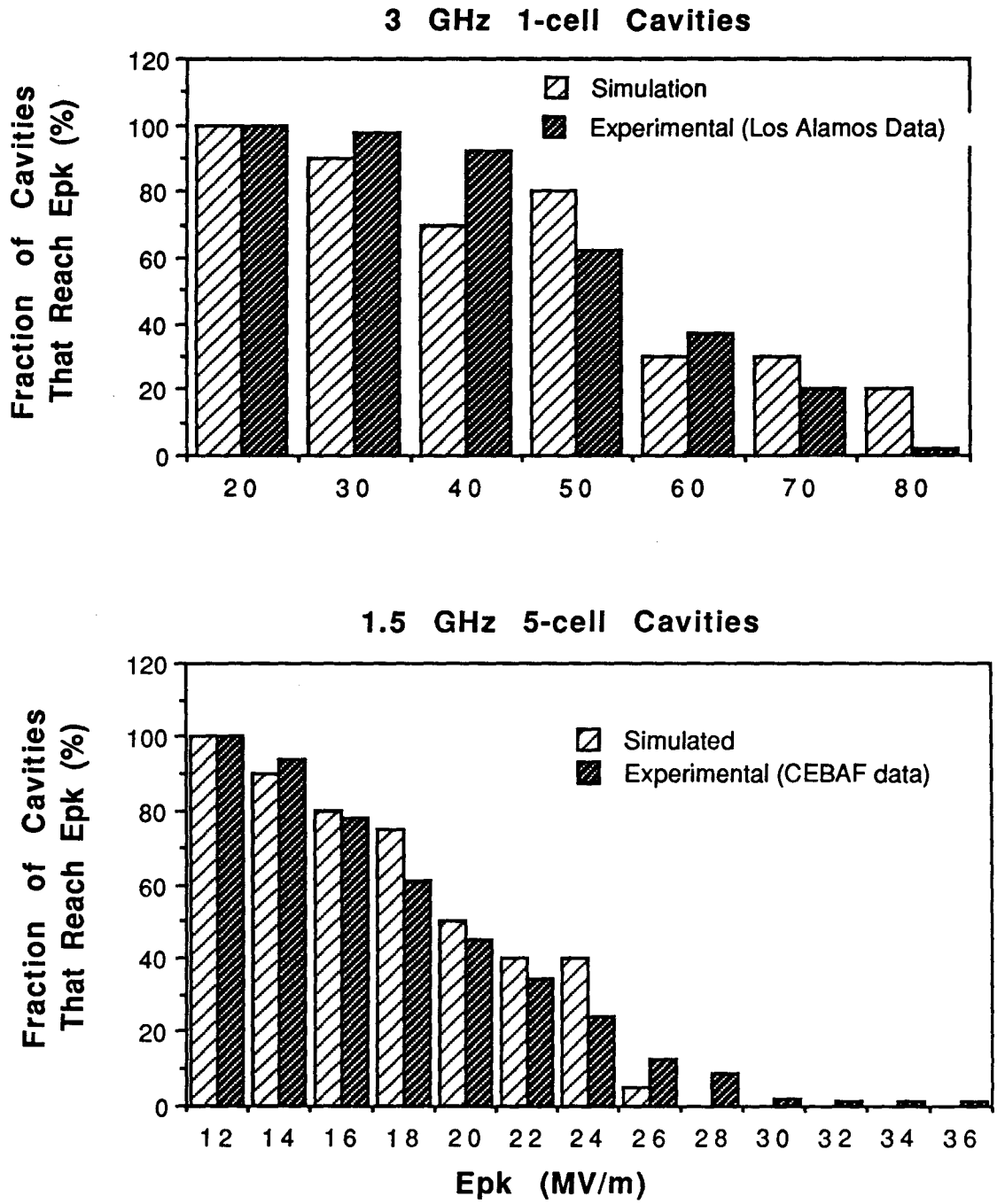

Figure 9: Comparision between predictions of the statistical model and experimental results for gradients achieved with 1-cell 3 GHz cavities (Los Alamos) and with 5-cell 1.5 GHz structures (CEBAF).

emitters. However for a 5-cell, 1.5 GHz cavity, the probability of exceeding even 30 MV/m is well below 20%.

The success of the simple statistical model points to the commonality of emitter properties and emitter density among cavities prepared by different laboratories. This is not very surprising, since we all use nominally the same chemical etching, rinsing, assembly and testing procedures. Only a radically different protocol of procedures is likely to affect emission.

Improved Cleanliness Approach

Over the last five years, increased vigilance in cleanliness of rinsing and assembly procedures has kept field emission at bay and brought us to the Eacc = 10 MV/m average performance level. What can we do to further increase cleanliness?

Heat Treatment at 1400 C

DC field emission studies[14,15] on cm^2 niobium samples have established the benefit of heat treatment above 1400 C. Single cell 1.5 GHz cavities heat treated to 1400 C, with titanium protection on the outside to preserve the RRR, have shown a statistically significant reduction in field emission as judged by thermometry based scans for the emitter density, as well as by examining the highest fields accessible[16]. In 10 tests, the average <Epk> was 50 MV/m, with 60 MV/m as the best case. (After heat treatment, these cavities were exposed to class 100 air, and rinsed with clean methanol to remove dirt introduced on removal from the furnace.) At Saclay, a 1-cell, 1.5 GHz cavity was heat treated in ring-like segments at 1700 C for 5 minutes in the electron beam welder. During heating, the inside was kept sealed under vacuum and the outside was coated with titanium. Without any further exposure, the cavity showed a flat Q vs E curve, at $Q = 10^{10}$, and Epk = 40 MV/m[8].

The data on heat treated multicells is still meager, and somewhat mixed. In three tests on heat treated 5- and 6-cell 1.5 GHz cavities at Cornell, we reached 15, 19.5 and 10 MV/m accelerating[17]. After careful efforts to clean the test set-up, 9-cell, 3 GHz heat treated cavities at Wuppertal reached 15 - 18 MV/m accelerating in three tests[18]. Again, thermometry based scans on the 9-cells show reductions in the overall density of sites, but

still the presence of one or two sites. Unfortunately, even a single "unprocessable" site can stop a cavity which may have an otherwise very clean surface. This is the important concern about the super-cleanliness approach.

High Pressure Water Rinsing

Another technique to improve cleanliness that is now increasing in popularity is high pressure water rinsing. Started at CERN[19], it is now being used at CEBAF[20], KEK[21] and Los Alamos[22]. In 10 tests on 1-cell, 1.5 GHz cavities at CEBAF, they reached <Epk> = 50 MV/m, with 64 MV/m as the best case. Several 5-cell cavities after high pressure rinsing reached the quench field without significant field emission. At Los Alamos, a 1-cell, 805 MHz cavity limited to Epk = 15 MV/m improved to 30 MV/m after 1 hour and to 50 MV/m after two hours high pressure rinsing. At CERN, high pressure rinsing was successfully used to recover a contaminated 1-cell, 350 MHz cavity which showed heavy field emission, to restore its peformance to Eacc = 12 MV/m. However other tests at CERN also showed that just clean water rinsing, without high pressure, is also successful in recovery, so the role of the high pressure is not clear in this case.

A useful technique to study the effectiveness of improved cleanliness strategies is to test their efficacy on silicon wafers that are subject to the same preparation steps as cavities[21,22]. The wafers are then scanned with a laser to study the particle density. High pressure water rinsing is found very effective in washing out particulate contaminants.

Yet another super-cleanliness approach, called sealed chemistry, is under development at Saclay[23]. The basic idea is to control the environment that the cavity surface is exposed to, so that it always sees only filtered acids, or filtered water or filtered air, and to automate all the preparation steps so that exposure to dust shed by humans is avoided. In three tests with 1-cell 1.5 GHz caviites, they reached Epk = 40 - 56 MV/m.

The Increased RF Processing Approach

In any of the super-cleanliness approaches, we can expect that the emitter density will be drastically reduced. Indeed thermometry based scans on heat treated surfaces show a factor of 10 reduction in emitter density[16]. However, even a single emitter can limit the

performance of the entire cavity, if it is unprocessable. There is always some probability, which is high for large area cavities, that one or two emitters will find their way in. Therefore, a technique that processes the remaining emitters in situ is highly desirable. Such a techinique will also be a weapon against accidental contamination of the cavity in an accelerator, or during assembly of couplers and other components. It is also clear how acute the need is for such an approach when we examine the experience of all laboratories that there is a decrease in performance between the acceptance or vertical cryostat test results and the in-tunnel test results.

The essential idea of High Pulsed Power (HPP) RF processing is to extend the RF processing of emitters by raising the surface field as high as possible, even if for a very short time. DC studies show spark formation times of < 1μsec[24]. The present level of understanding that has emerged from our HPP studies is that, as the field is raised, the strongest emitters put out so much field emission current, that a micro-discharge, or RF spark takes place, and the ensuing explosive event processes the offending emitter. When the field level is raised further, the next strong emitters will process, and so on.

To illustrate this sequence of events, Figure 10 shows the thermometry identification of an emitter at Epk (CW) = 31.7 MV/m. After processing with HPP at Epk(pulsed) = 49 MV/m, the emission was reduced as shown by maps at Epk(CW) = 32.3 and 33.6 MV/m. Further HPP at Epk(pulsed) = 54 MV/m drastically reduced emission as shown by the temperature map at Epk(CW) = 36.3 MV/m. After dissection of the cavity, SEM/EDX examination of the projected emitter location revealed the feature shown in Figure 11. It is believed that the starburst is the result of the plasma activity associated with the discharge, most likely a cleaning of the surface, either from electron or ion bombardment. At the core of the spark, the heating is sufficiently intense to intiate melting and cratering. The debris of Figure 11 was analyzed by X-ray spectra to reveal titanium, calcium, carbon and oxygen.

Other than providing the high power to reach a high Epk in the presence of heavy field emission and falling Q_0, it appears that there is no fundamental difference in the processing mechanism between HPP and CW RF. An isolated CW RF processing event in a 1-cell 3 GHz cavity was captured with thermometry and further analyzed by microsocopy[8]. Figure 12 shows Q vs.E curves, temperature maps and the SEM picture for the CW processing event at Epk(CW) = 30 MV/m. EDX analysis of particulate matter in the crater region revealed

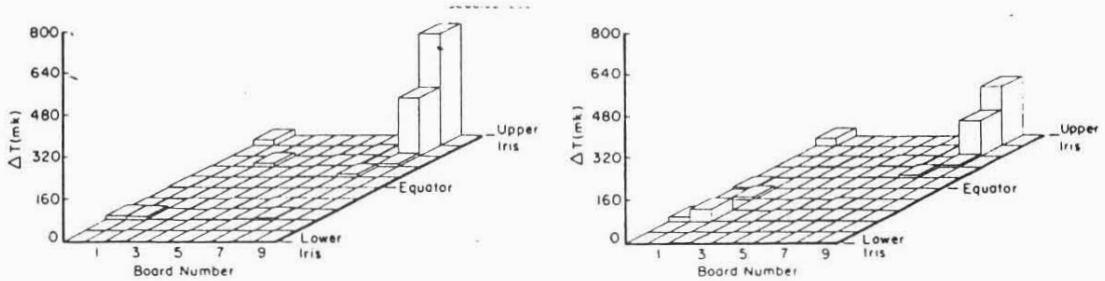

(a). Initial Rise; E_{peak} = 31.7 MV/m. (b). After HPP; E_{peak} = 32.3 MV/m.
HPP :P_{inc} = 2 kW, $E_{peak} \leq$ 49 MV/m.

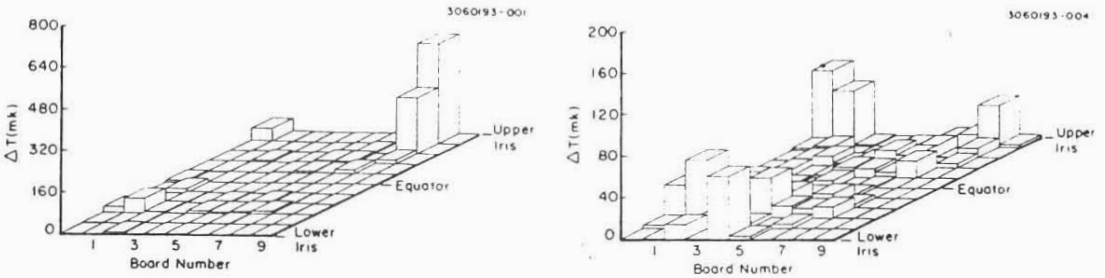

(c).After HPP; E_{peak} = 33.6 MV/m. (d). 2nd HPP; E_{peak} = 36.3 MV/m.
HPP: P_{inc} = 3.5 kW, $E_{peak} \leq$ 54 MV/m

Figure 10: Temperature maps showing the processing of an emitter with HPP at various field levels.

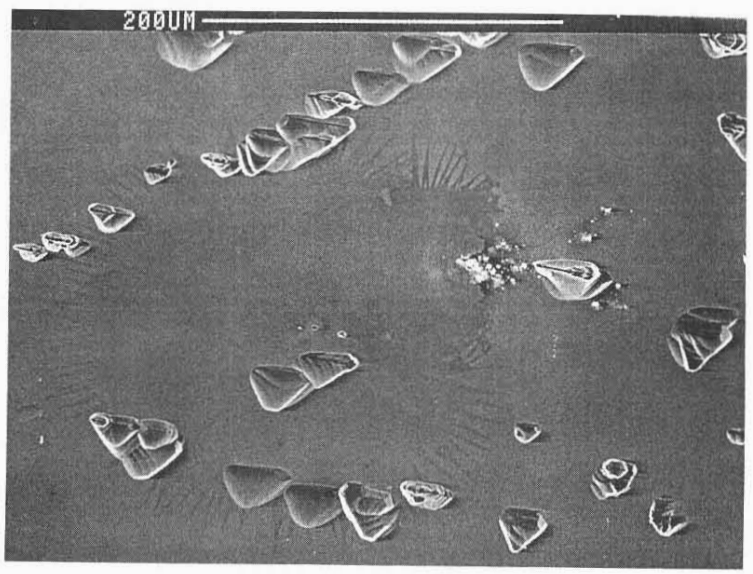

Figure 11: Microscopic examination of emission site after HPP RF processing studied in Figure 10.

copper as the contaminant element for this site. All the molten craters and starburst routinely observed in the mushroom cavity were obtained after CW RF processing.

The performance improvement of Nb cavities with HPP has been throughly demonstrated. More than 25 HPP tests have been carried out with 1-cell, 2-cell, 5-cell and 9-cell cavities at 3 GHz[8] and at 1.3 GHz[25]. Figure 13 shows the best result with a 9-cell, 3 GHz cavity and the best result with a 5-cell, 1.3 GHz cavity. Here the Q vs E of the cavities are shown both before HPP and after HPP to demonstrate the large range of the overall improvement. Note that the TESLA goal of Eacc = 25 MV/m has been reached for the 5-cell, 1.3 GHz cavity.

All the CW results from 8 tests on two 9-cell cavities are shown in Figure 14, again both before and after HPP. In each case the cavities started out with a freshly treated chemically etched surface. In each case heavy field emission was successfully processed with HPP to reach Eacc = 15 - 20 MV/m. The results after HPP are plotted as a function of the maximum Epk achieved during the pulsed processing stage. The mechanisms responsible for limiting of the highest Epk reachable both in the CW and in the pulsed stage are discussed in another section.

All the results from 6 tests on three 5-cell, 1.3 GHz cavities are shown in Figure 15, plotted in the same way. We include one test on a 2-cell, 1.3 GHz cavity in the same plot. Again, for each test, the surface of the cavity was freshly prepared by etching. In all but one case we reached Eacc = 16 - 32 MV/m after HPP, if we use the ratio Epk/Eacc = 2, as for the TESLA shape cavity.

Strong evidence that the effectiveness of the processing depends on the maximum Epk reached during the pulsed stage emerges from tests on 1-cell, 3 GHz cavities as well as tests on a 2-cell cavity as depicted in Figure 16. The reason that the 2-cell performed much better than the 1-cells will be discussed in the next section.

Effectiveness of HPP against new field emission from vacuum accidents.

The benefit of HPP remains when the cavities are exposed to filtered N2 or filtered air, as proven with both the 9-cell, 3 GHz as well as with the 5-cell, 1.3 GHz cavities, both at

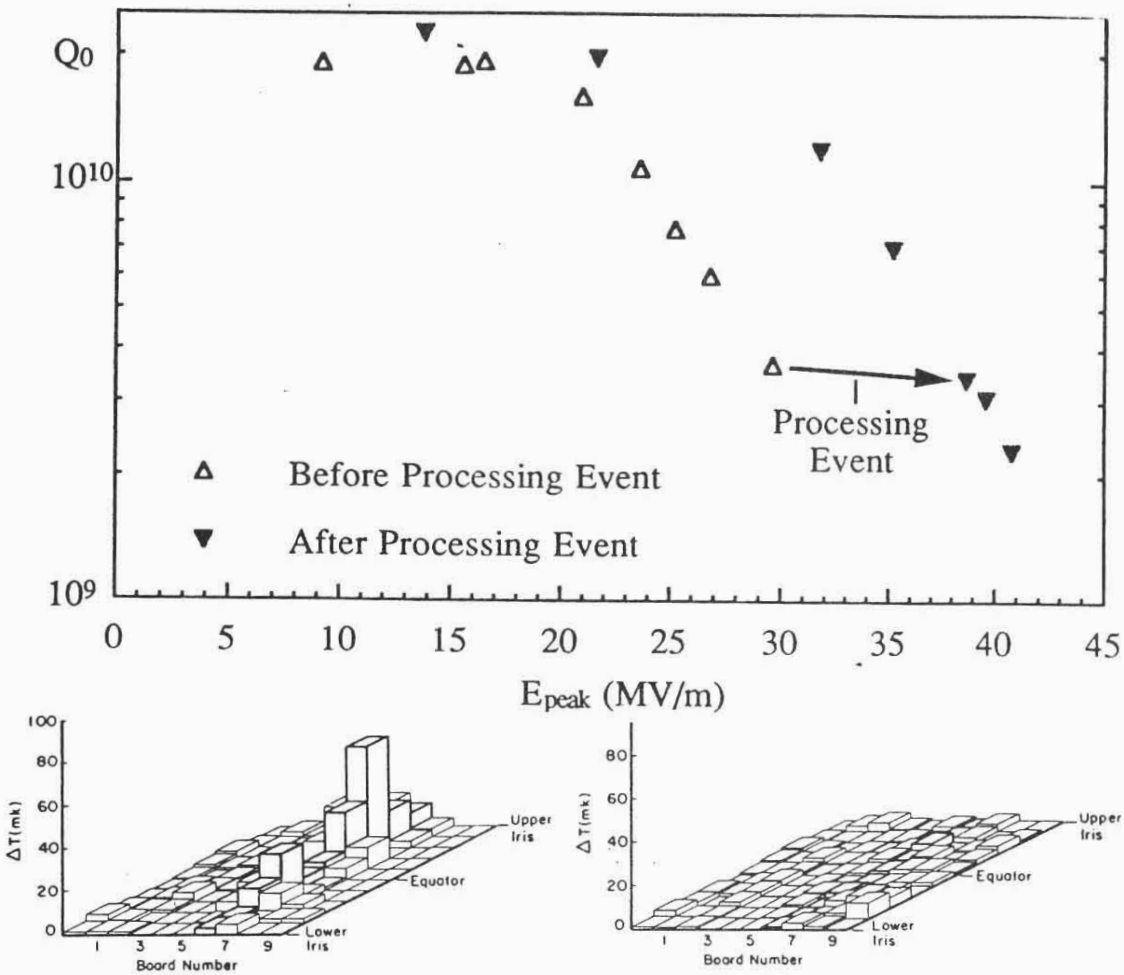

(a). Before low power event; E_{peak} = 29.6 MV/m.

(b). Following low power event; E_{peak} = 31.7 MV/m.

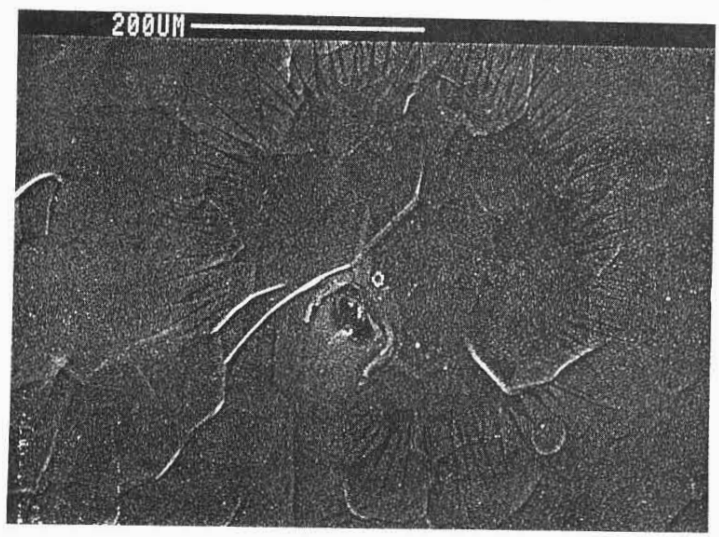

Figure 12: (Top) Q vs E curve for a CW RF processing event. (Middle) Temperature maps before and after processing. (Bottom) Microscopic information on emission site after CW RF processing

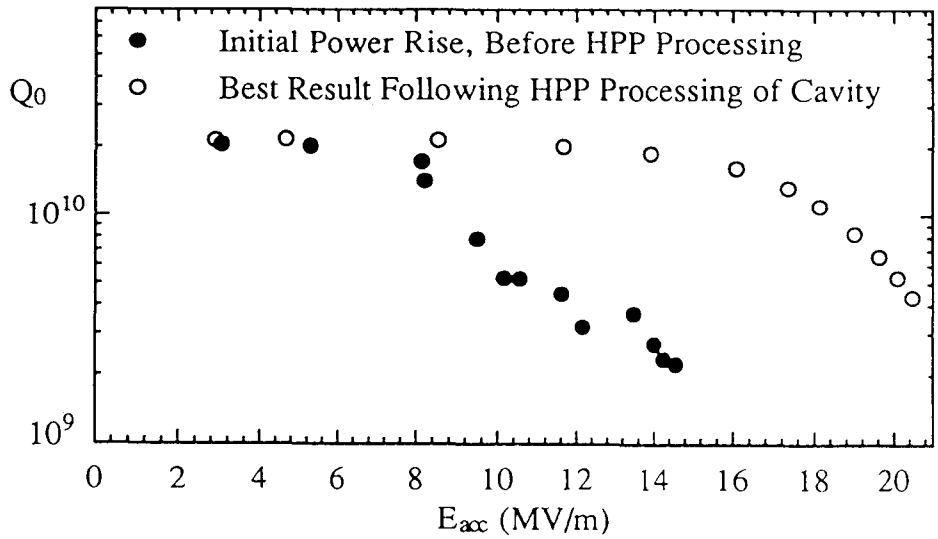

Figure 13: (Top) Best result from HPP processing a 9-cell 3 GHz cavity. (Bottom) Best result from HPP processing of 5-cell 1.3 GHz cavity.

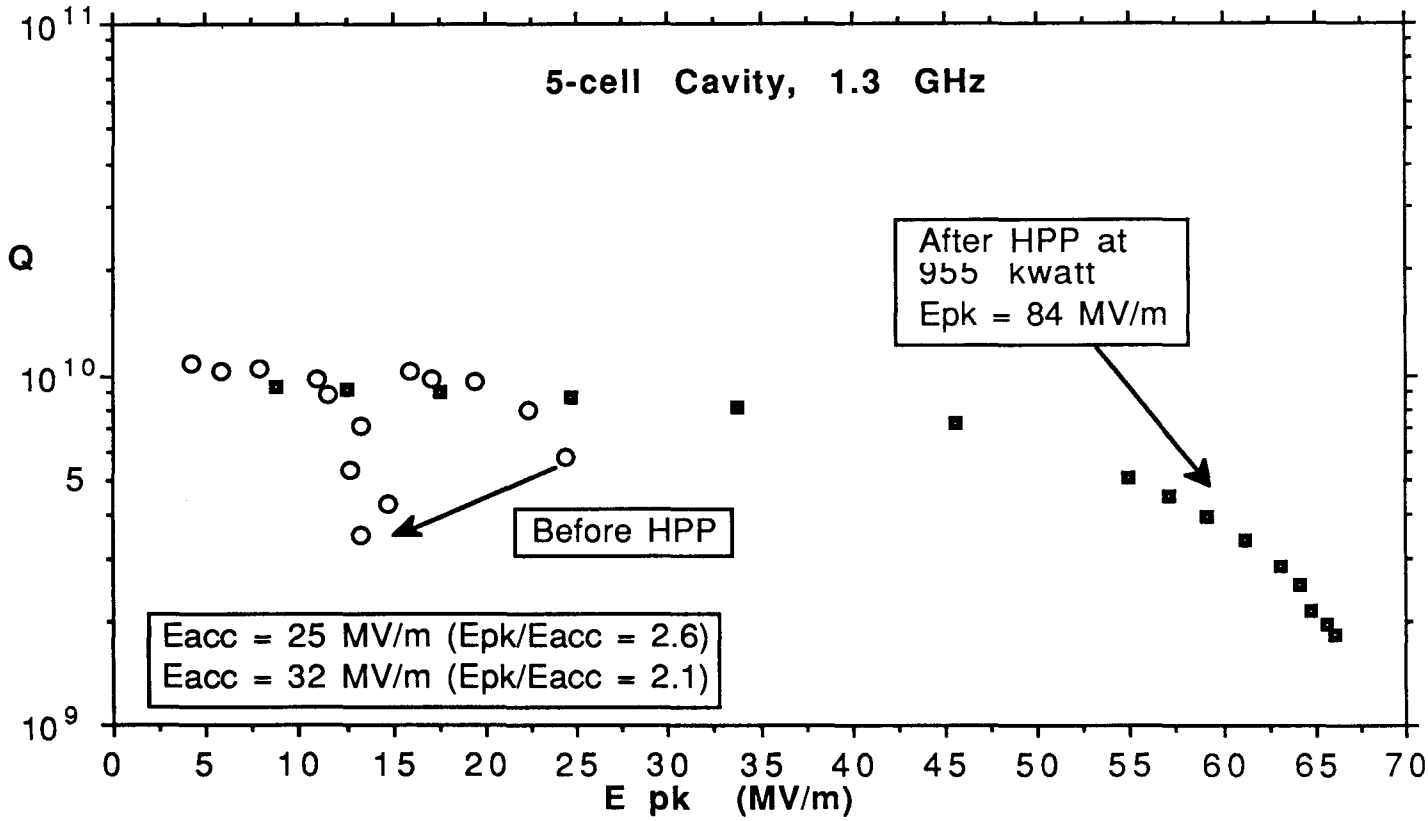

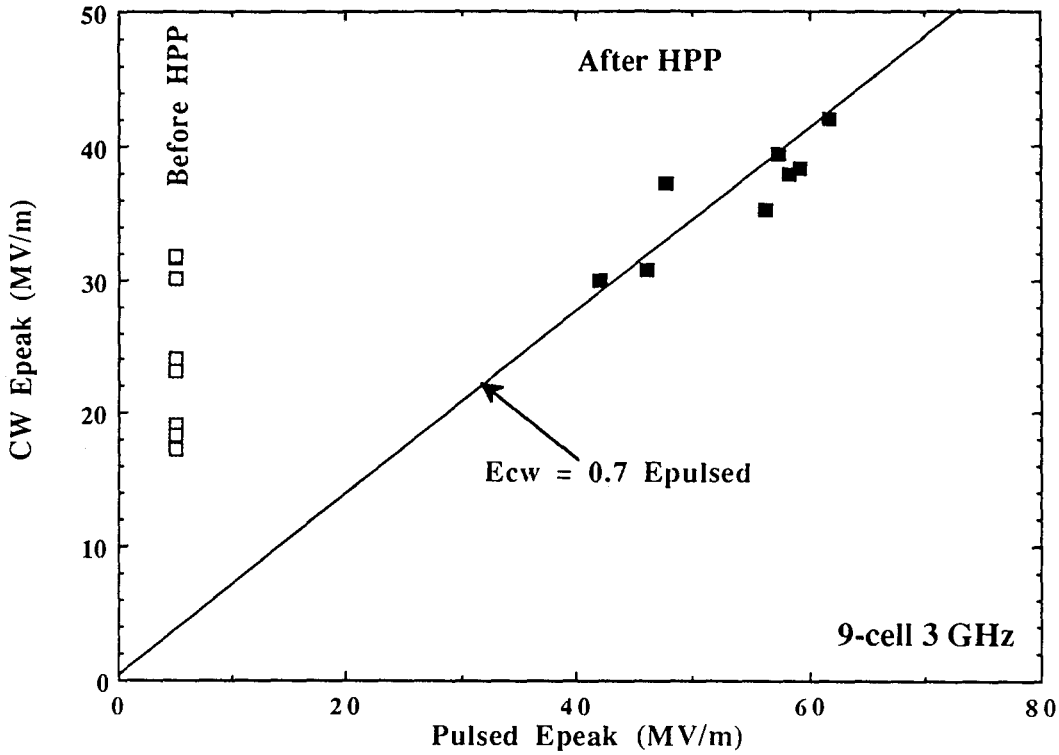

Figure 14: HPP improvement from 8 tests on two 9-cell 3 GHz cavities.

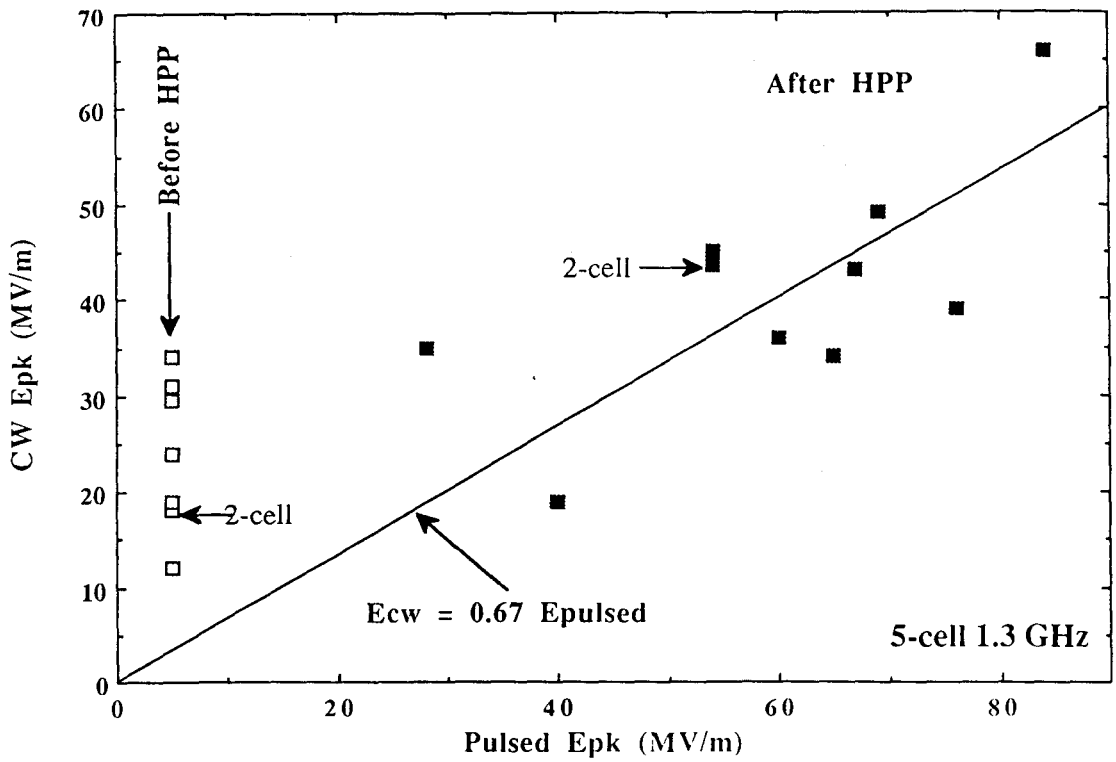

Figure 15: HPP improvement from 5 tests on three 5-cell 1.3 GHz cavities and one 2-cell 1.3 GHz cavity.

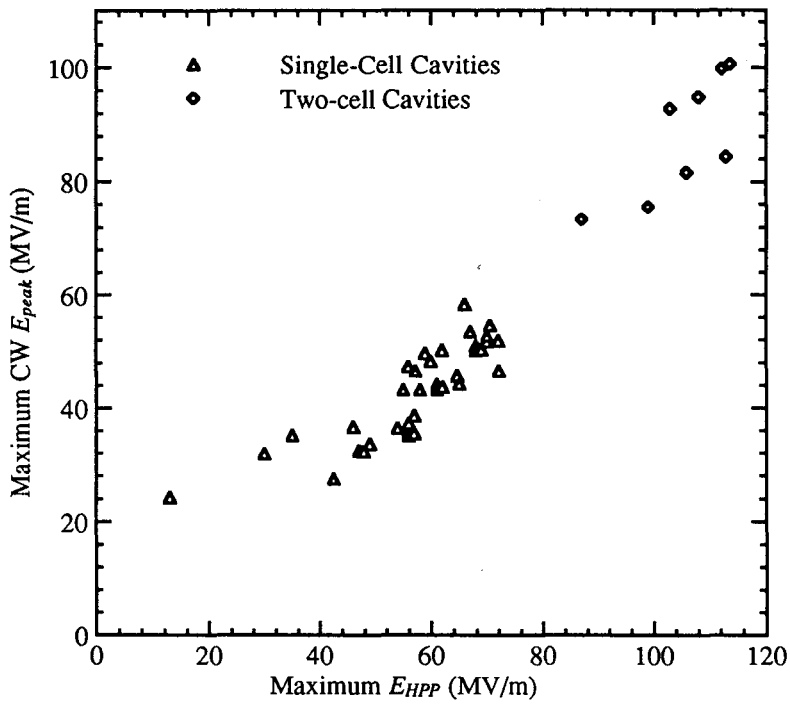

Figure 16: Correlation between E (CW) and E(pulsed) for 1-cell and 2-cell 3 GHz cavities.

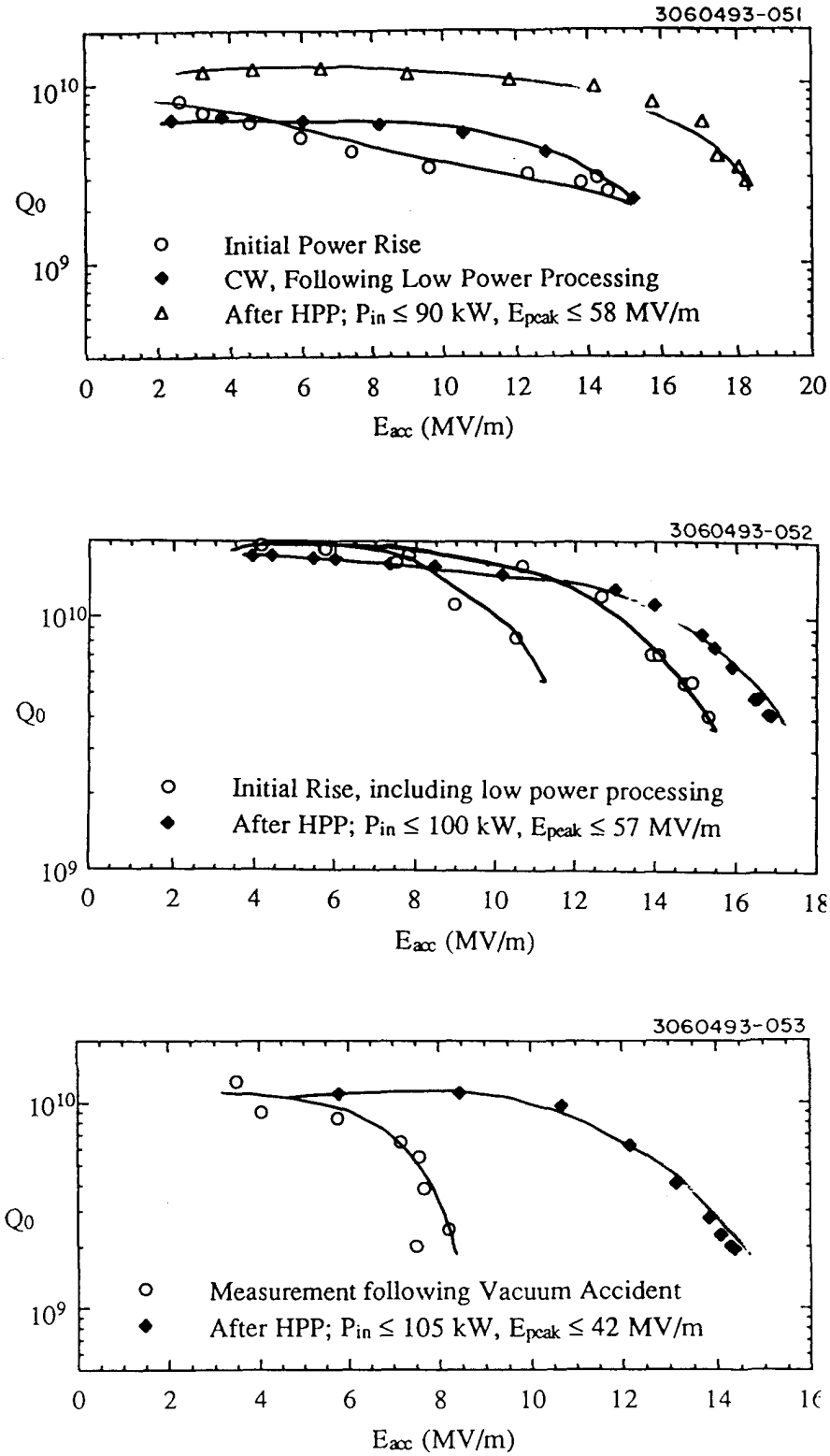

Figure 17: Effectiveness of HPP for recovery from field emission contaminants introduced in vacuum accidents.

Eacc max = 18 MV/m. We arranged three accidents with varying degrees of severity, as shown in Figure 17[8]. In the mildest case, the accident was a few torr of air from a rouging pump line to a cold cavity. The low power Q dropped from $2x10^{10}$ to $7x10^{9}$. Without warming, HPP recovered the low power Q to $1x10^{10}$, and processed field emission to reach Eacc = 18 MV/m. In a warm accident, we bled up the same cavity to one atmosphere of dirty room air. After pump out and cool down, the field emission was already intense at Eacc = 10 MV/m, but was processed by a combination of CW and HPP to Eacc = 17 MV/m (Figure 17 - middle panel). Finally we let up the same cavity to 1/2 atmosphere of dirty room air while cold, warmed up the cavity and cooled down. Now the emission was intense at Eacc = 8 MV/m, but again successfully processed by HPP to Eacc = 15 MV/m. The in situ processing capability is therefore strongly verified.

Limitations of the HPP method

In the pulsed stage, the maximum Epk reached depends on the:

a) power available
b) pulse length
c) power that can be successfully coupled through the processing coupler to the cavity
d) Qext of the coupler and
e) Q_0 of the cavity at the high field.

(a) and (b) depend on the performance of the klystron and modulator systems. c) depends on the high power capability of the coupler and windows, as well as the success in conditioning the coupler. d) depends on the range of adjustability of the coupling probe e) depends on how much the Q_0 falls due to intensifying field emission currents as well as due to any growing normal conducting regions, if thermal breakdown starts.

If the cavity is dirty, then the power consumed by emission may cause the Q_0 to fall too much during HPP, limiting Epk. Therefore cleanliness is important to get the best results from HPP. If the cavity has a low RRR, or a significant defect, then thermal breakdown will limit the pulsed Epk, (at least for long pulse lengths) to the same level as the CW Epk. To raise Epk beyond the CW breakdown level, it is necessary to raise the power faster than the growth of the normal conducting region, which requires substantial power. This technique

has indeed been successfully used [26] to reach fields 40% higher than the CW breakdown field with 150 kwatts into a 1-cell 3 GHz cavity.

Another thermal breakdown limitation can arise from global thermal instability over large portions of the RF surface[8]. In this mechanism both the residual resistance and the exponentially increasing BCS surface resistance play the dominant role, rather than defects. Comparing the temperature map (Figure 18) just below breakdown for the two types of thermal breakdowns shows the local vs the broad nature of the heating. At 3 GHz, thermal modelling calculations show that the global thermal instability will set in at 1400 Oersted for residual $Q = 10^{10}$.

Lowering the RF frequency to 1.3 GHz, as for TESLA, eliminates the global thermal type of instability as the BCS resistance drops with f^2. Another way is to lower the ratio of Hpk/Epk, so that higher Epk can be accessed for processing away emitters. Unfortunately, the geometries explored so far also raise Epk/Eacc, so that the utility of this approach is purely for improved understanding. It is important to prove in principle that the benefits of field emission processing continue as Epk rises. Following this line, we made a 2-cell cavity of the spherical shape used by Wuppertal, for which Hpk/Epk drops from 20 to 14 Oersted/MV/m but Epk/Eacc = 2.9. Figure 16 shows how the benefits of HPP indeed extend out to 100 MV/m.

Using typical numbers for a) through e), Figure 19 shows the calculated maximum Epk possible for a 9-cell cavity with 150 kwatts and several pulse lengths from 0.1 msec to 0.5 msec. Here we assume that the Q_0 stays at 3×10^6 throughout the pulse, which is pessimistic, since the Q_0 falls to its lowest value only at the highest field, due to one or several of the mechanisms described above. We also show in Figure 20 the calculated Epk with 1 Mwatt for a pre-TESLA 5-cell 1.3 GHz cavity of the type being tested at Cornell and for a 9-cell TESLA cavities soon to be tested at DESY. For the 1.3 GHz cases, we assume Q_0 falls to 2×10^6. Such calculations prepare us for the power, pulse lengths and coupling ranges necessary.

To process away field emission we must reach a high Epk-pulsed. But to avoid thermal breakdown we must have a high RRR. Figure 21 shows the progress made with a 1.3 GHz 5-cell cavity by attacking both fronts[25]. The cavity started with RRR = 300. In the top

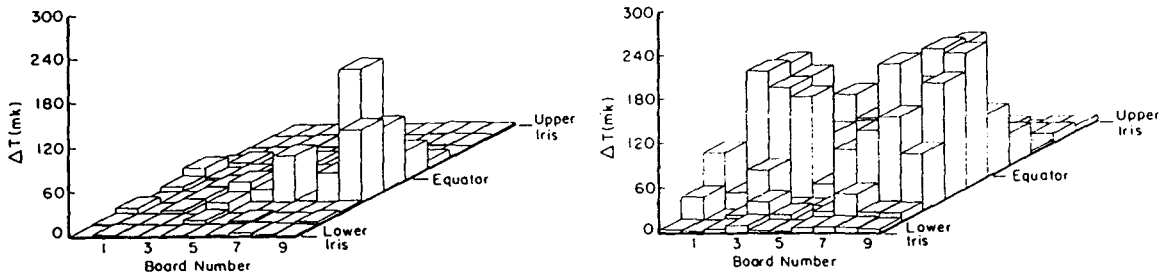

(a) Defect Breakdown (b) GTI Breakdown

Figure 18: Temperature maps below breakdown comparing local thermal breakdown with global thermal breakdown in a 1-cell 3 GHz cavity.

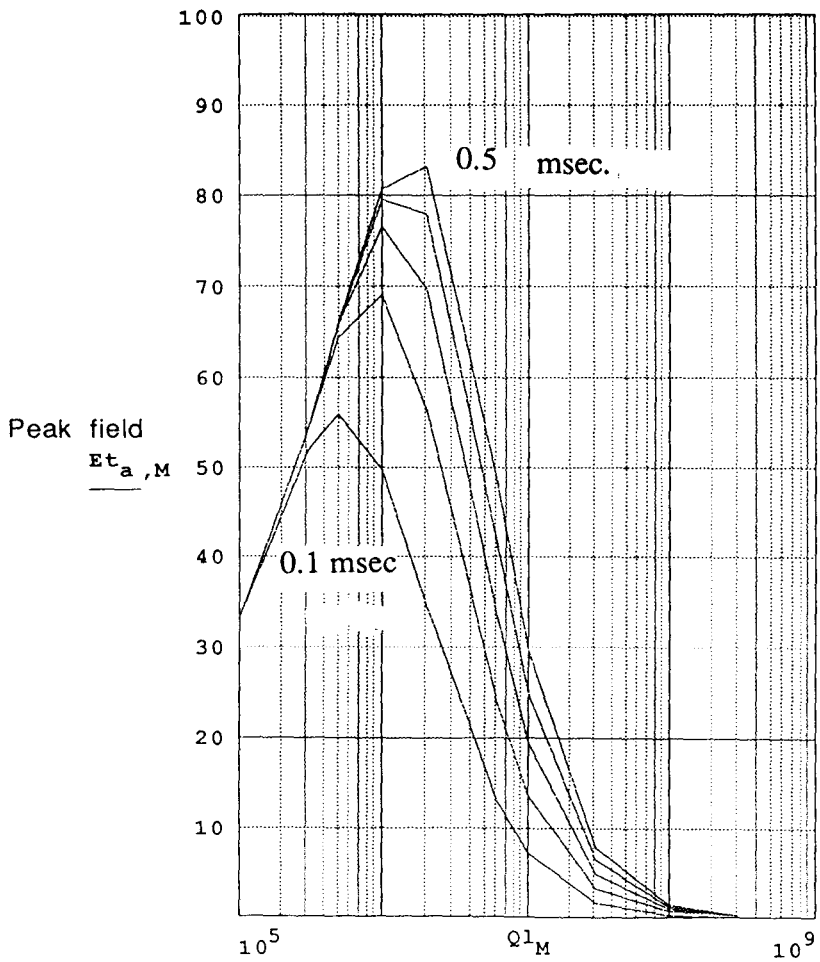

Figure 19: Calculated values for surface fields that can be reached in a 9-cell 3 GHz cavity with 150 kwatts power for various pulse lengths and Qext, assuming Q_0 is 3×10^6 throughout the pulse.

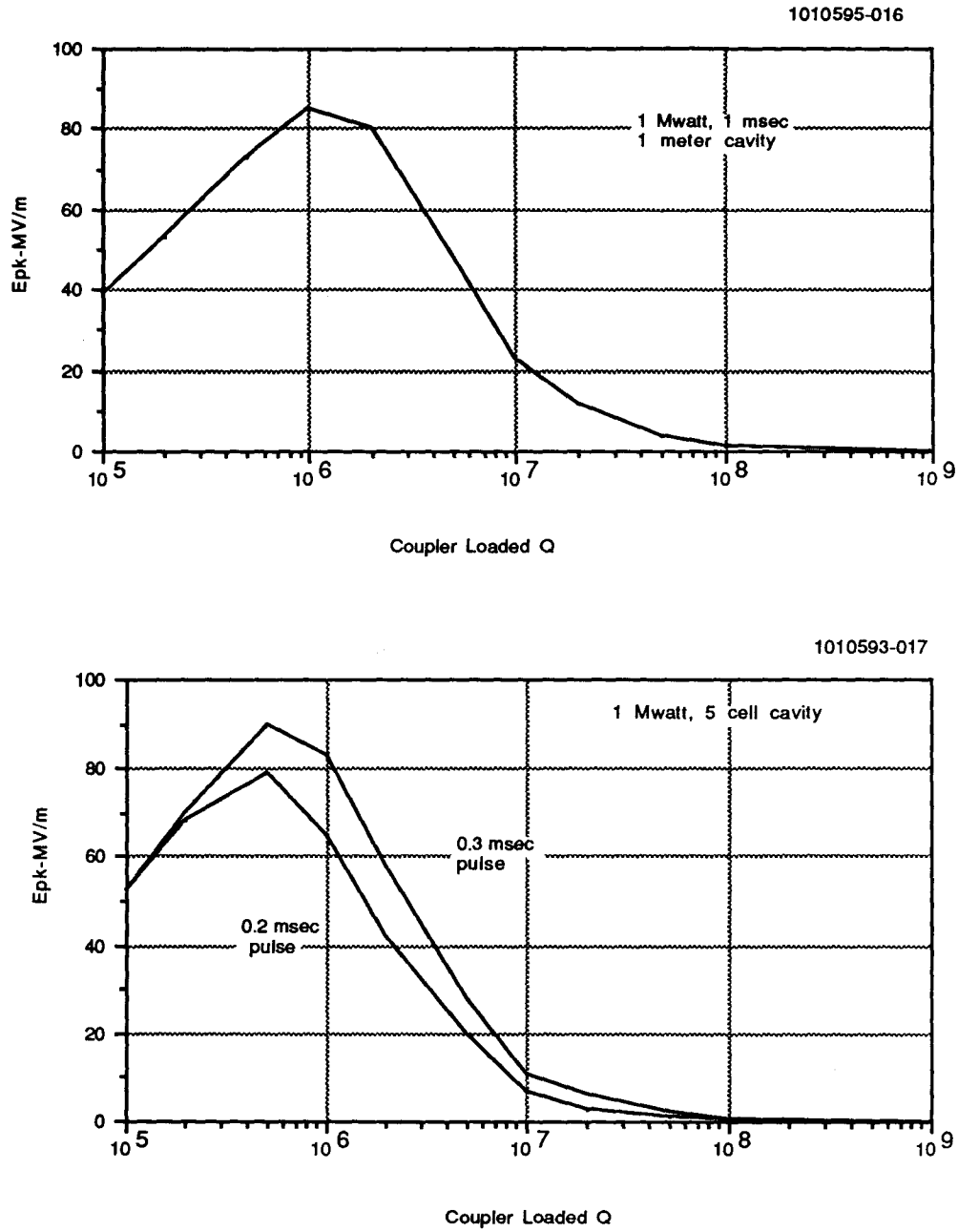

Figure 20: Calculated values for surface fields that can be reached in 1.3 GHz cavities (a)9-cells and (b) 5- cells with 1 Mwatt RF power for various pulse lengths and Qext, assuming Q_0 is $2x10^6$ throughout the pulse.

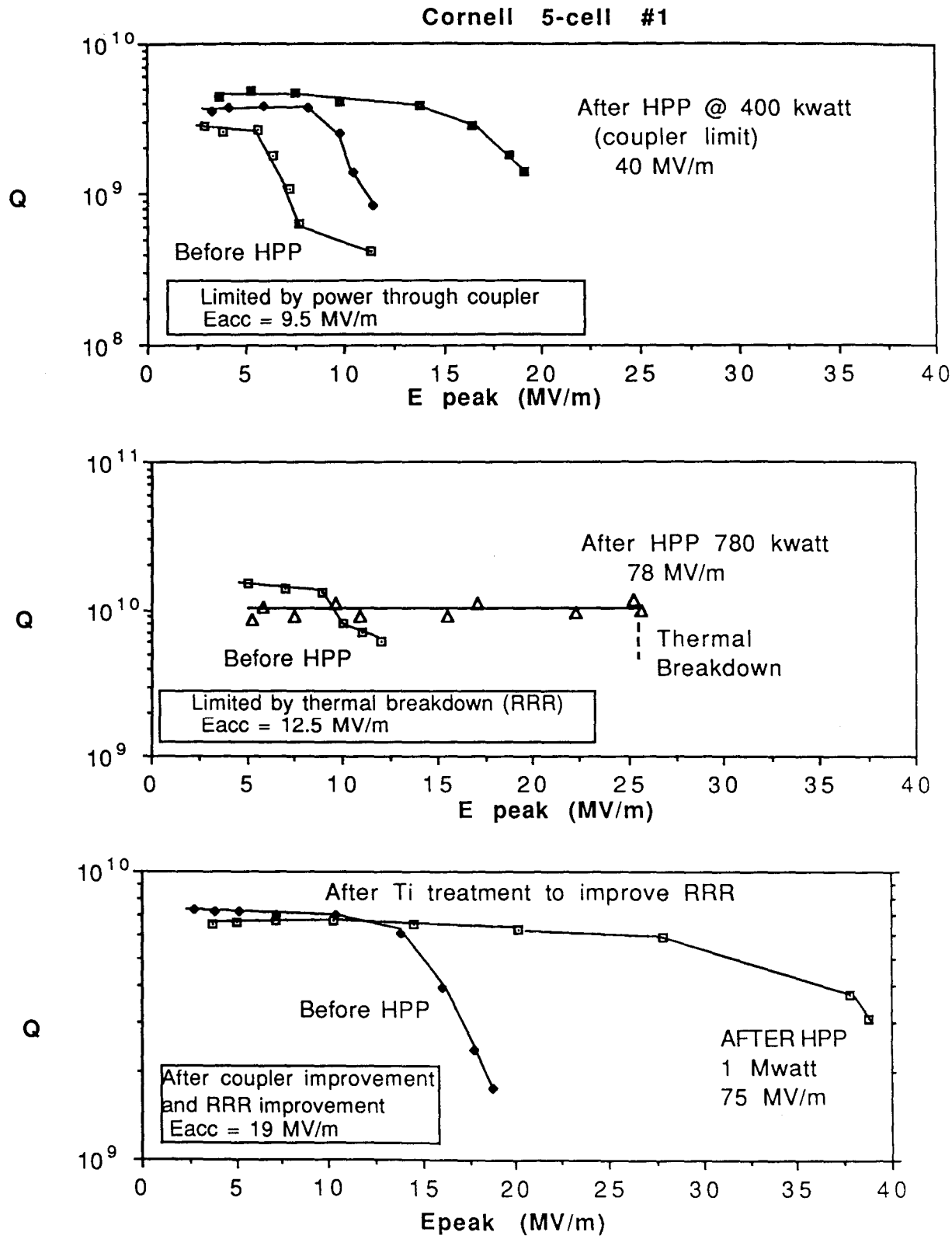

Figure 21: Progress in achievable fields with increasing power for processing field emission and increasing RRR to avoid thermal breakdown.

panel, the cavity was limited by field emission to CW-Epk = 19 MV/m because the maximum processing power was limited by coupler breakdown to 400 kwatts. In the middle panel, we improved the coupler design so processing could extend to 780 kwatt. Now thermal breakdown limited the cavity, after emission was processed at 78 MV/m using 780 kwatt. In the bottom panel the RRR was improved by at least a factor of 2 using inside/outside Ti treatment. Now HPP with 1 Mwatt at 75 MV/m made it possible to reach CW- Epk = 40 MV/m, corresponding to Eacc = 20 MV/m.

Conclusions

The present surface preparation techniques are adequate for the Q values we need for TESLA. To achieve the high gradients needed, the three basic parameters to control are: the RRR of the niobium to avoid thermal breakdown, cleanliness to avoid field emission, and the power delivered to the cavity for high pulsed power processing of residual emission. Systematic application of this understanding has repeatedly led to CW Epk = 30 - 66 MV/m in multi-cell cavities which translates to Eacc = 15 - 32 MV/m for TESLA structures. For the future we need to continue to push toward RRR = 1000 to ensure thermal stability. Still to be proven is how far in situ HPP can be used with the fixed input coupler intended for operation with beam.

References

[1] C. Reece et al, 1993 Particle Accelerator Conference, Washington DC.
[2] R. Roeth et al, 5th Workshop on RF Superconductivity, Hamburg.
[3] R. Roeth et al, 1992 EPAC, Berlin.
[4] D. Reschke et al, this conference.
[5] P. Kneisel et al, this conference.
[6] G. Muller, Uni. Wuppertal, private communication.
[7] R. Noer et al, this conference.
[8] J. Graber, PhD Thesis, Cornell University.
[9] D. Moffat et al, 5th Workshop on RF Superconductivity, Hamburg.
[10] T. Hays et al, this conference.
[11] Ph.Niederman, Ph.D. Thesis, University of Geneva.
[12] H. Padamsee et al, 1993 Particle Accelerator Conference, Washington DC.
[13] B. Rusnak et al, 1992 Linac Conference, Chalk River.
[14] E. Mahner et al, this conference.
[15] Ph. Niedermann et al, Third Workshop on RF Superconductivity, Argonne.
[16] H. Padamsee, et al, 4th Workshop on RF Superconductivity, KEK.
[17] J. Kirchgessner et al 1993 Particle Accelerator Conference, Washington DC.
[18] D. Reschke et al, this conference.
[19] D. Bloess, CERN, private communication.
[20] P. Kneisel et al, this conference.
[21] K. Saito et al, this conference.
[22] B. Rusnak, Los Alamos, private communication.
[23] B. Bonin et al, this conference.
[24] G. A. Mesyats, IEEE Trans. Electrical Insulation, EI-18, 218 (1983) & B. Juttner IEEE Trans. Plasma Science, PS-15, 474 (1987).
[25] C. Crawford et al, this conference.
[26] J. Graber et al, this conference.